Global Journal of Engineering and Technology Advances

eISSN: 2582-5003

Cross Ref DOI: 10.30574/gjeta

Journal homepage: https://gjeta.com/

Global Journal of Engineering and Technology Advances
eISSN: 2582-5003
Global Scholar Press, INDIA

(REVIEW ARTICLE)

Check for updates

Rotman lens: Systematic review of simulation approaches

Mohammed K. Al-Obaidi [1, 2, *]

[1] *University Tun Hussein Onn Malaysia, 86400 Parit Raja, Batu Pahat, Johor, Malaysia.*
[2] *College of Engineering, Computer Engineering Department, Al-Iraqia University, Baghdad, Iraq University Tun Hussein Onn Malaysia, 86400 Parit Raja, Batu Pahat, Johor, Malaysia.*

Global Journal of Engineering and Technology Advances, 2022, 11(03), 079–085

Publication history: Received on 17 May 2022; revised on 22 June 2022; accepted on 24 June 2022

Article DOI: https://doi.org/10.30574/gjeta.2022.11.3.0098

Abstract

The beamforming technique is an important factor in designing modern wireless communications systems. While Rotman lens is a vital method to achieve the ability to steer the radiation pattern at the desired locations. Besides, there are many contributions to enhancing the performance of such lens, however, a classification to review this development is required. The main objective in this study objective is to explain and discuss the historical evolution of the Rotman lens as a beamformer based on the simulation methods used to analyze the mathematical model of the Rotman lens. The study shows that the variety of the methods is to achieve accurate simulation results while the simulation time and hardware computer requirements are still a challenge.

Keywords: Rotman lens; Fullwave simulations approaches; Electrically large and complex structure; Beamforming

1. Introduction

Rotman lens was created as a beamforming network (BFN) in the 1963s and was then used in numerous cutting-edge applications [1]. Rotman lens beamformer works on the assumption of geometric optics. Typically, such a beamforming network is used for a wide-band frequency operation[2], 5G wirelss system[3],and 6G applications [4]. The schematic drawing of a two-dimensional Rotman lens is shown in Figure 1. Where N is referred to the adjacent elements distance and Y is the receive distance from the x-axis. The beam port part includes several radiators in the transmission mode, and it works as receiving radiator in the receiving mode. Besides, each radiated beam is related to an input port. The array port surface consists of several receiving elements that are linked to the array elements through different length transmission lines to save the linearity of phase shifting.

The principle of operation in order to generate the out beam in the desired direction can be explained as follow. The excitation is applied to the beam port. Each receiving port directs the received energy from the beam port to the element in the array port. The phase of the received signal is directly proportional to the path length (travelling distance) between the beam port radiator and the receiving element. This model produces a linear phase shift across the radiator elements. Thus, each beam port element is related to a beam at a unique scan angle.

Many researchers are motivated to implement a Rotman lens to control the produced beam in the desired location. In radar surveillance systems, these lenses are usually used to see objectives in various directions owing to their multibeam capacity without physically shifting the antenna structure. In the following, the main properties of the microstrip Rotman lens will be described.

* Corresponding author: Mohammed K. Al-Obaidi: Al.obaidi.m.k.i@gmail.com
Universiti Tun Hussein Onn Malaysia, 86400 Parit Raja, Batu Pahat, Johor, Malaysia.

The structure of the Rotman lens is derived from the geometric optic theory [1][5]. Therefore, the linear phase-shifting reached to the radiator elements is based on the different path lengths taken by the feeding signal to reach each element. Besides, its ability to generate multiple beams based on the concept of geometrical optics theory on other words, the location of the beam port, receiving port, radiator element, focal length, and the transmission line length produce the true time delay (TTD)[6][7]. Therefore, the produced beam scan angle is based on the path length difference without using a line coupler compared to the Butler matrix beamforming circuit [8][9]

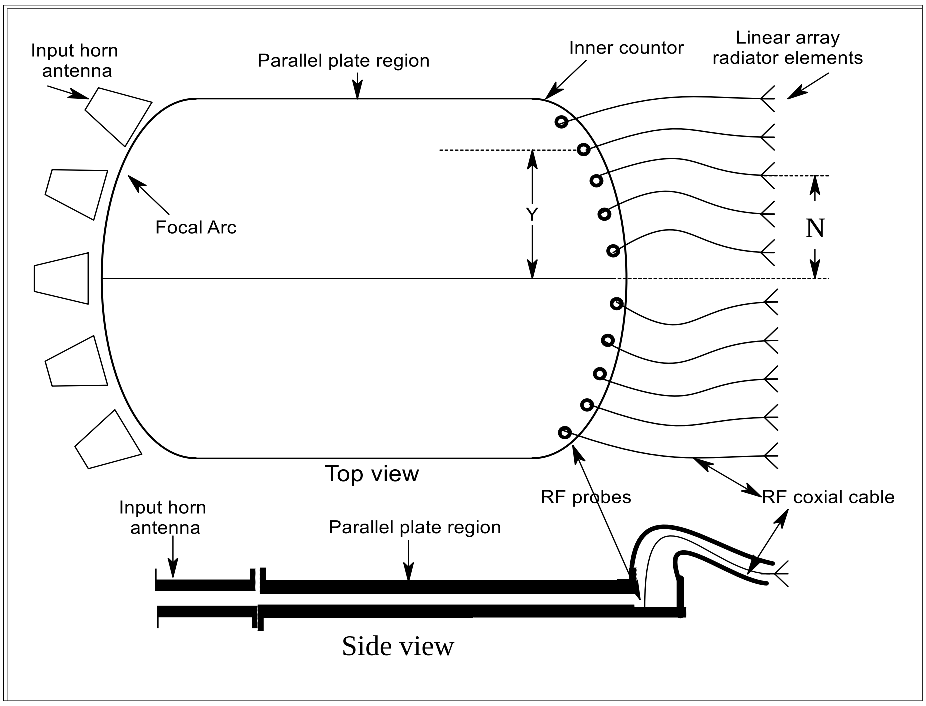

Figure 1 Schematic original Rotman lens [1]

While Blass matrix is a beamforming circuit that is made up of several wave supply lines linked by rows with the linear array [10].

2. Microwave lens: a brief review of developments history

The microwave lens is the device that can generate multiples beams to scan the desired angle. Since 1946, the formulation of a microwave lens has started from evolving the geometric optics technique adopting in microwave applications such as concave parabolic antenna and lens antenna [11]. Numerical simulation methods development

Precise analysis of Rotman lens must include computing the complete scattering lens matrix in terms of mutual coupling with internal reflections between feed ports, return loss, and phase coupling. Furthermore, the most common lens feed port and substrate configurations can be included. An analysis using fully rigorous methods such as Method of Moment (MoM), Finite Element (FE), Finite-difference Time Domain (FDTD) may not be feasible due to the wide electrical area on the lens (typically over 100 square wavelengths) [12]. In the following, the development of the numerical approaches used in the performance analysis calculations of the lens is explained.

2.1. Ray structure method

This approach is based on the calculation of coupling coefficients for each unique ray introduced by the source and interacts with the receiving elements, as explained in Figure 2. Then, the sum of these rays is close to the modal results [13].

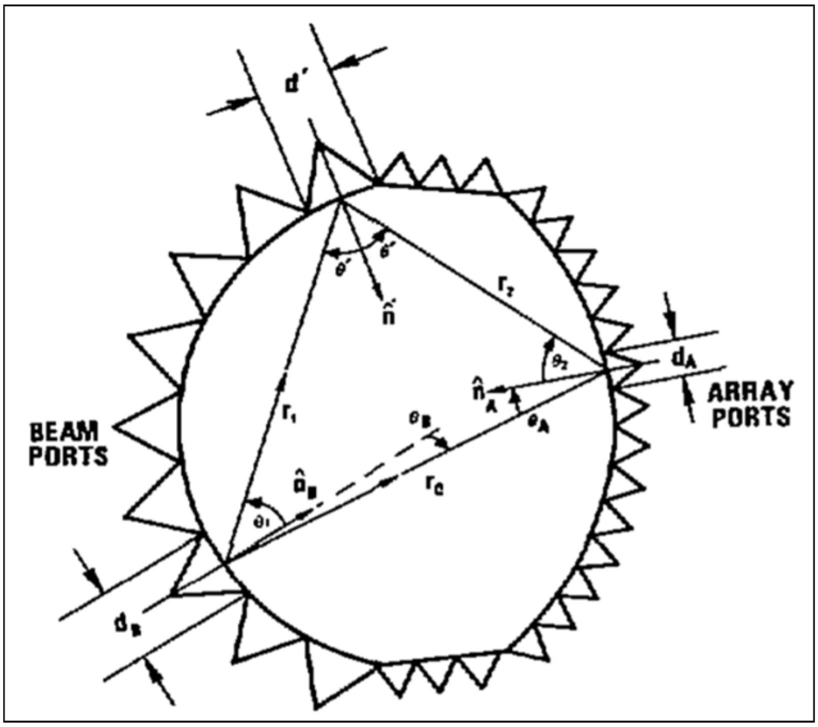

Figure 2 Ray structure method explanation [13]

The coupling coefficients of the direct ray path $S^0_{A,B}$ generated from the source port and the reflected ray path coefficient $S^1_{A,B}$ can be determined from the following equations:

$$S^0_{A,B} = \sqrt{\frac{2\pi d_A d_B}{Kr_0}} \frac{E(\theta_A, d_B) E(\theta_A, d_A)}{\lambda} e^{-jkr_0} \quad (1)$$

$$S^1_{A,B} = \sqrt{\frac{2\pi d_A d_B}{K(r_1 + r_2)}} \frac{E(\theta_1, d_B) E(\theta_2, d_A)}{\lambda} \Gamma\left(\bar{\theta}, \bar{d}\right) e^{-jk(r_1 + r_2)} \quad (2)$$

Where K is the wavenumber, λ is the wavelength inside the parallel plate of the lens cavity, d_A is the width of the wave ports, and d_B is the beam ports width. While, E(θ, d) is the radiation pattern of the port has width d and the angle θ normal to the port and $\Gamma(\bar{\theta}, \bar{d})$ is referred to the active voltage reflection inside the lens inner junction has an angle equal to $\bar{\theta}$. The method is proved the ability to calculate the coupling magnitude besides the phase coupling for the Rotman lens has 100 beam ports and 188 array ports at 10 GHz. However, more accuracy is needed for the determined results compared to full-wave simulation approaches while this method is considering the initial step to developing the hybrid ray-tracing approach, as it will be explained in the following section.

2.2. Contour boundary integral hybrid function

A full-wave method of moment technique (MoM) for ports that properly account for the fringed areas is used in this technique [14]. Besides, The Rao, Wilton and Glisson (RWG) triangle subdomain features are embedded, which can fit any multi-faceted port form [15]. Also, a broadband description of the stripline prospective features of the Green function is used, which numerically efficiently allows rigorous port assessment [16]. The approach is applied and validated by implementing it to prototype Rotman lens has 46 beam ports and 41 array ports in [17] and approved the accuracy besides the fast simulation time.

2.3. Least-squares finite element method (LSFEM)

A combination method combining the least-squares finite element technique (LSFEM) and the transfinite element approach is used to evaluate Rotman lens performance [18]. Using the LSFEM allows the process to yield both the distribution of electromagnetic fields in the lens structure and the commuting of the scattering matrix. The analysis technique starts to partition the structure of a Rotman lens into two main parts, the part of discontinuity due to impedance mismatching (including the region of the lens and the tapered microstrip lines) and the semi-infinite port area. The proposed method is based on solving first-order Maxwell equations because of the approximation of microstrip and strip Rotman lens as a planar multiport network structure. The proposed approach is examined to model a prototype microstrip lens 9×8 input-output ports, and it provides an accurate result which agrees with measurement results. The technique is suggested to be embedded in computer-aided software; furthermore, it can be extended to simulate a full-wave three dimensions environment as future work.

2.4. Domain decomposition and distributed analysis

A domain decomposition method that decreases the memory needed to compute major finite element issues is outlined [19][20]. It includes dividing a sizeable computational domain into several smaller subdomains and iteratively resolving the subdomain issues, as shown in Figure . While the subdomains are separated using Robin boundary conditions to guarantee the correct field between them [21]. Compared to the existing domain solution, the memory demands of the entire solution process are significantly decreased. Although, the full CPU time needed to solve the complete lens is larger than the full domain algorithm for the domain decomposition alternative. While it is considered more efficient to work in network parallel computer mode, this mode is used to solve the large computational problem, especially when a high memory random access memory (RAM) is required.

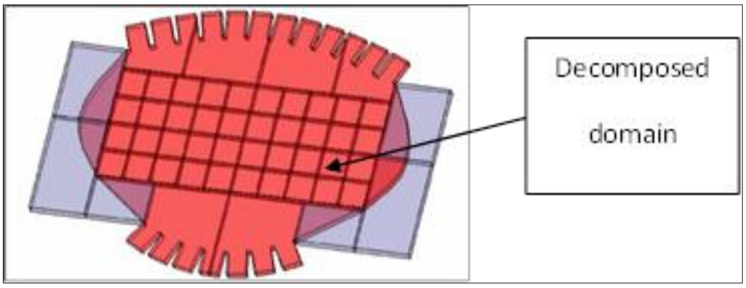

Figure 3 Domain decomposition technique applied to Rotman lens [19]

Besides, the number of calculation iterations needs to be reduced, especially to calculate the Z matrix, which is referred to the subdomain one time only. Therefore, this feature is suggested as future work.

2.5. Hybrid ray tracing method

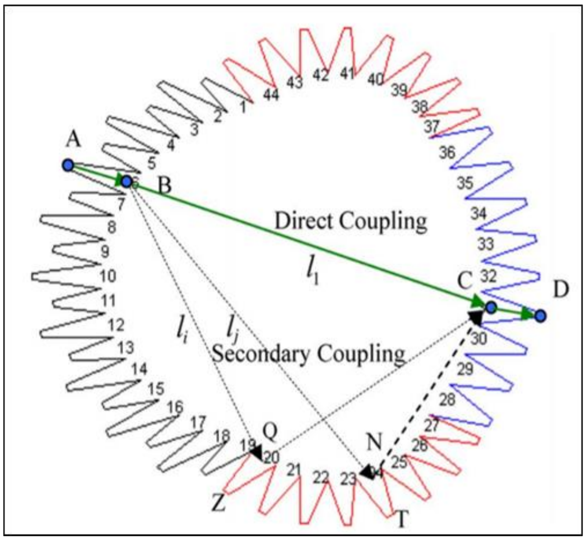

Figure 4 Fast hybrid tracing for Rotman lens modelling [22]

A fast and straightforward ray tracing algorithm is suggested for the microwave lens design. The proposed technique constructs the lens structure and tests its performance in terms of the tapered ports, phase, and energy coupling between ports, besides the construction of the transmission line [22]. The proposed method is considered an extension for the work reported in [13] in terms of accuracy and less return loss ports. The approach is based on the modelling of the lens by multipath ray tracing using hybrid and more flexible port analyzing, as shown in

Figure .

The validation of the ray trace approach is carried out by comparing the predicted results to the full-wave simulation results and the measurement results. This approach can achieve a fast simulation environment. However, the amplitude of the apertures for the edge ports shows a somewhat more significant error value than full-wave models and measures outcome, mainly because of irregular edge port constructions and alignment. Furthermore, phase centre estimation can be adopted to the approach to increase the accuracy of the phase prediction results. Besides, the method can be introduced as a toolkit to build a fast and accurate lens model.

2.6. Two-dimensional finite difference time domain (2D-FDTD) approach

The finite-difference time-domain (FDTD) approach is one of today's most common electromagnetic problem-solving techniques. It has been implemented to a wide range of issues, such as the calculation of scattering parameters for metal and dielectrics, antennas, microstrip circuits, and electromagnetics. Fast and accurate microstrip Rotman lens geometry is modelled using two dimensions finite difference time domain is reported in [23]. Furthermore, the model to estimate the conductor loss is proposed to provide more design accuracy. The suggested technique is based on solving Maxwell equations for the components as described in the following equations:

$$\begin{cases} \varepsilon \dfrac{\partial E_y}{\partial t} = \dfrac{\partial H_x}{\partial z} - \dfrac{\partial H_z}{\partial x} \\ \mu \dfrac{\partial H_x}{\partial t} = \dfrac{\partial E_y}{\partial z} \\ \mu \dfrac{\partial H_z}{\partial t} = \dfrac{\partial E_y}{\partial x} \end{cases} \quad (3)$$

The proposed method was implemented to microstrip Rotman lens while the proposed method was contributed for saving the simulation time compared to another approach, as explained in the below table:

Table 1 Comparative of time simulation for numerical methods [23]

Solution type	Number of mesh cell	Simulation time
HFSS (FEM)	1 236 676	3.5 hours
(3D-FDTD)	5 145 008	4 hours
(2D-FDTD)	218 346	4 min.

Long time saving for the proposed method can be indicated in Table . However, the proposed method is applied for the microstrip Rotman lens, and more investigation can be carried out to extend its work to other Rotman lenses, such as strip and waveguide models.

3. Conclusion

A review of the numerical simulation approaches used to solve Rotman lens mathematical model is discussed in this study. The comparison between types is based on the mathematical model and the simulation time. Besides, the requirements of the computer hardware are discussed. Full-wave simulation approaches provide more accurate results for the Rotman lens model. However, the complexity and the simulation time must be considered.

Compliance with ethical standards

Acknowledgments

All authors whose work where used in this present work are specially acknowledged and appreciated. This work received no funding from external sources.

Disclosure of conflict of interest

The authors declare that they have no known competing financial interests or personal relationships that could have appeared to influence the work reported in this study.

References

[1] W Rotman, R Turner. Wide-angle microwave lens for line source applications, IEEE Transactions on Antennas and Propagation. Nov. 1963; 11(6): 623–632.

[2] F Cardoso, S Matos, J Costa, C Fernandes, J Felicio, NJG Fonseca. Design of a Rotman Lens Operating in the Full K/K a Band Using Ridge Waveguide Technology. 2022; 1–5.

[3] A Eid, J Hester, MM Tentzeris. Extending the Range of 5G Energy Transfer: Towards the Wireless Power Grid. 1–May 2022; 4.

[4] U Nissanov. 6G Rotman lens D-band beam-steering microstrip antenna, Journal of Computational Electronics 2022; 21(2): 431–444.

[5] H Hong et al. Ka-Band Rotman Lens-Based Retrodirective Beamforming System for Wireless Power Transfer, jees.kr. 2022.

[6] R Rotman, M Tur, L Yaron. True Time Delay in Phased Arrays, Proceedings of the IEEE. 2016; 104(3): 504–518.

[7] Y Gao, M Khaliel, F Zheng, T Kaiser. Rotman Lens Based Hybrid Analog Digital Beamforming in Massive MIMO Systems: Array Architectures, Beam Selection Algorithms and Experiments," IEEE Transactions on Vehicular Technology. 2017; 66(10): 9134–9148.

[8] Y Liu, C Liu, X Liu, X Yang. Circularly polarized beam-steering antenna array for ultra-high frequency radio frequency identification applications, International Journal of RF and Microwave Computer-Aided Engineering. 2019; 29(10): 1–8.

[9] B Cetinoneri, YA Atesal, GM Rebeiz. An 8×8 Butler Matrix in 0.13-μmCMOS for 5–6-GHz Multibeam Applications," IEEE Transactions on Microwave Theory and Techniques. 2011; 59(2): 295–301.

[10] P Chen, W Hong, Z Kuai, J Xu. A Double Layer Substrate Integrated Waveguide Blass Matrix for Beamforming Applications, IEEE Microwave and Wireless Components Letters. Jun. 2009; 19(6): 374–376.

[11] WE Kock. Metal-Lens Antennas, Proceedings of the IRE. 1946; 34(11): 828–836.

[12] MJ Maybell, KK Chan, PS Simon. Rotman lens recent developments 1994-2005, in 2005 IEEE Antennas and Propagation Society International Symposium. Jul. 2005; 2B: 27–30.

[13] M Maybell. Ray structure method for coupling coefficient analysis of the two dimensional Rotman lens. in 1981 Antennas and Propagation Society International Symposium. Jun. 1981; 19: 144–147.

[14] AF Peterson, EO Rausch. Validation of integral equation model with high-dielectric microstrip Rotman lens measurements," in Proceedings of the 1991 Antenna Applications Symposium. 1991; 208–229.

[15] S Rao, D Wilton, A Glisson. Electromagnetic scattering by surfaces of arbitrary shape," IEEE Transactions on antennas and propagation. 1982; 30(3): 409–418.

[16] WF Richards, K Mcinturff, PS Simon. An efficient technique for computing the potential Green's functions for a thin, periodically excited parallel-plate waveguide bounded by electric and magnetic walls, IEEE Trans Microw Theory Tech. 1987; 35(3): 276–281.

[17] P Simon. Analysis and synthesis of Rotman lenses, in 22nd AIAA International Communications Satellite Systems Conference and Exhibit 2004 (ICSSC). 2004; 1–11.

[18] AJ Parfitt. Analysis of Rotman lenses using a hybrid least squares FEM/transfinite element method," IEE Proceedings - Microwaves, Antennas and Propagation. 2001; 148(3): 193–198.

[19] Longtin MC, Sun DK, Silvestro J, Cendes Z. Domain Decomposition and Distributed Analysis for Large Microwave Structures. In2006 IEEE MTT-S International Microwave Symposium Digest 2006 Jun 11 (pp. 1053-1056). IEEE.

[20] J Silvestro, M Longtin, Din-Kow Sun, Z Cendes. Rotman lens simulation using the finite element domain decomposition method," in 2005 IEEE Antennas and Propagation Society International Symposium, Jul. 2005; 2B: 47–50.

[21] S Alfonzetti, G Borzi, N Salerno. Iteratively-improved Robin boundary conditions for the finite element solution of scattering problems in unbounded domains," International Journal for Numerical Methods in Engineering. 1998; 42(4): 601–629.

[22] J Dong, AI Zaghloul. Hybrid Ray Tracing Method for Microwave Lens Simulation, IEEE Transactions on Antennas and Propagation. 2011; 59(10): 3786–3796.

[23] SMR Vaziri, AR Attari. An improved method of designing optimum microstrip Rotman lens based on 2D-FDTD, International Journal of RF and Microwave Computer-Aided Engineering. 2019; 30: 1–12.